KSME International Journal, Vol. 17 No. 10, pp. 1533~1542, 2003

The Study on Pressure Oscillation and Heat Transfer Characteristics of Oscillating Capillary Tube Heat Pipe

Jong-Soo Kim*
School of Mechanical Engineering, Pukyong National University,
San 100, Yongdang dong, Nam-gu, Pusan 608-737, Korea
Ngoc Hung Bui
Graduate student, School of Mechanical Engineering, Pukyong National University,
San 100, Yongdang dong, Nam-gu, Pusan 608-737, Korea
Hyun-Seok Jung
Samsung Electronics Co. Ltd, 416, Maetan-3Dong,
Paldal-Gu, Suwon City, Kyungki-Do, 442-742, Korea
Wook-Hyun Lee
Korea Institute of Energy Research.,
71-2, Jang-Dong, Yuseong-Gu, Daejeon 305-343, Korea

In the present study, the characteristics of pressure oscillation and heat transfer performance in an oscillating capillary tube heat pipe were experimentally investigated with respect to the heat flux, the charging ratio of working fluid, and the inclination angle to the horizontal orientation. The experimental results showed that the frequency of pressure oscillation was between 0.1 Hz and 1.5 Hz at the charging ratio of 40 vol.%. The saturation pressure of working fluid in the oscillating capillary tube heat pipe increased as the heat flux was increased. Also, as the charging ratio of working fluid was increased, the amplitude of pressure oscillation increased. When the pressure waves were symmetric sinusoidal waves at the charging ratios of 40 vol.% and 60 vol.%, the heat transfer performance was improved. At the charging ratios of 20 vol.% and 80 vol.%, the waveforms of pressure oscillation were more complicated, and the heat transfer performance reduced. At the charging ratio of 40 vol.%, the heat transfer performance of the OCHP was at the best when the inclination angle was 90°, the pressure wave was a sinusoidal waveform, the pressure difference was at the least, the oscillation amplitude was at the least, and the frequency of pressure oscillation was the highest.

Key Words : Oscillating Capillary Tube Heat Pipe (OCHP), Pressure Oscillation, Frequency, Power Spectrum

Nomenclature

f : Frequency, [Hz]
p : Pressure, [kPa]
q : Heat flux, [W/cm^2]

* Corresponding Author,
E-mail : jskim@pknu.ac.kr
TEL : +82-51-620-1502; **FAX** : +82-51-611-6368
School of Mechanical Engineering, Pukyong National University, San 100, Yongdang dong, Nam-gu, Pusan 608-737, Korea. (Manuscript **Received** March 2, 2001; **Revised** September 27, 2002)

Greeks

α : Charging ratio, [vol.%]
θ : Inclination angle, [°]
λ : Thermal conductivity, [W/mK]

Subscripts

eff : Effective
eva : Evaporating part
cond : Condensing part

1. Introduction

Heat pipe is a very effective device for transmitting heat with high rates over considerable distances with extremely small temperature drops, exceptional flexibility, simple construction, and easy control with no external pumping power. There are various parameters that limit the rate of heat transport through heat pipes. The capillary limit is the most commonly encountered limitation in the operation of heat pipes. It occurs when the capillary pumping rate is not enough to provide liquid to the evaporating part. This is due to the fact that the sum of the liquid and vapor pressure drops exceeds the maximum capillary pressure that the wick can sustain. The entrainment limit is due to the influence of the shear force which exists at the liquid-vapor interface (Faghri, 1995). The capillary and entrainment limits are overcome by using the oscillating capillary tube heat pipe (OCHP).

The OCHP is a very promising heat transfer device (Akachi, 1994). In addition to its excellent heat transfer performance, it has a simple structure: in contrast with conventional heat pipes, there is no wick structure to return the condensed working fluid back to the evaporating part. The OCHP is made from a long continuous capillary tube bent into many turns of serpentine structure. The working fluid is charged into the OCHP. The diameter of the OCHP must be sufficiently small so that vapor plugs can be formed by capillary forces. The OCHP is operated within a 0.1~5 mm inner diameter range. The OCHP can operate successfully for all heating modes. The heat input, which is the driving force, increases the pressure of the vapor plugs in the evaporating part. In turn, this pressure increase will push the neighboring vapor plugs and liquid slugs toward the condensing part, which is at a lower pressure. However, due to the continuous heating, bubbles are endlessly formed by nucleate boiling in the evaporating part. The bubbles grow and coalesce to become vapor plugs. The flow of vapor plugs and liquid slugs moves to the condensing part by the pressure difference between the evaporating part and the condensing part. The heat transfer continuously occurs. As a result, thermal energy is rapidly transferred from the evaporating part to the condensing part as well as the oscillation and the circulation of vapor plugs and liquid slugs occurring in the OCHP (Izumi et al., 1998; Kim et al., 1999; Lee et al., 1999a, 1999b).

Both experimental and numerical investigations on the OCHP have been carried out by some researchers to determine the pressure mechanism governing the flow of working fluid in the OCHP. Miyazaki and Akachi (1996) studied the pressure oscillation characteristics of the OCHP with respect to the variations of heat flux and charging ratio. They observed the movement phenomena of oscillation wave of long liquid slugs and vapor plugs and proposed an analytical model based on these phenomena. They concluded that the heat transfer performance was improved when the amplitude of pressure oscillation decreased and the frequency of pressure oscillation increased. Suzuki (2000) also studied the temperature oscillation characteristics of a copper-water oscillating capillary heat pipe. The frequency of temperature oscillation was found and a proportional relation between effective thermal conductivity and frequency was proposed.

Although some experimental evidence suggested the correlation between the pressure oscillation and heat transfer characteristics in the OCHP, studies related to the characteristics of pressure oscillation with respect to the variation of heat flux, the charging ratio of working fluid, and the inclination angle were not found. It was the aim of the present work to make clear the effect of pressure oscillation characteristics on the heat transfer performance of the OCHP.

2. Experimental Apparatus and Methods

The schematic diagram of the experimental apparatus was shown in Fig 1. It consists of a test section, data acquisition system, heating system, and circulation system of cooling water. The test section was manufactured to the serpentine structure with fine flow channels on the surface

of a brass plate. The length of the channel was 220 mm. Each channel cross-section was rectangular with a width of 1.5 mm and a height of 1.5 mm. For visualization of the internal flow of the OCHP, the test section was covered with transparent acryl and tightened with bolts. The test section was formed by 10 turns (20 channels) of the looped type. The detailed specifications of the test section were represented in Fig. 2. The data acquisition system was divided into a temperature and pressure measuring system. Each measuring system was composed of a data logger and personal computer. The heating system was an electrical heater plate of which the heat input was adjusted by using a voltage regulator and digital power meter. The circulation system of cooling water was composed of a constant temperature bath and volumetric flow meter. The cooling water circulated through the test section, the volumetric flow meter, and the constant temperature bath.

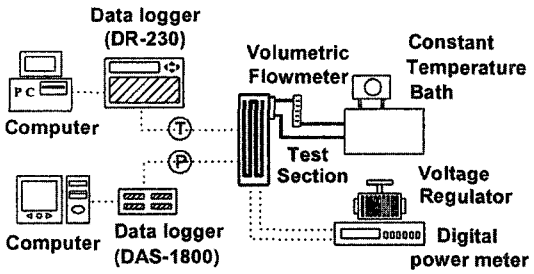

Fig. 1 The schematic diagram of the experimental apparatus

The locations of thermocouples for measuring the surface temperature of the test section were shown in Fig. 3. Three holes of a 1.1 mm diameter were perforated into the center of the test section across and under 1 mm from the bottom of the channels. Three holes were located at the evaporating, the adiabatic, and the condensing part, respectively. A sheath type thermocouple of a 1.0 mm diameter was inserted and sealed into each hole. To minimize the contact resistance between

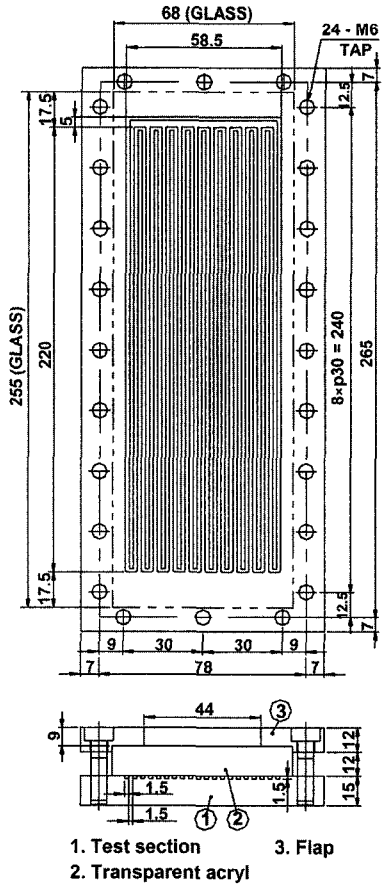

Fig. 2 Specifications of the test section

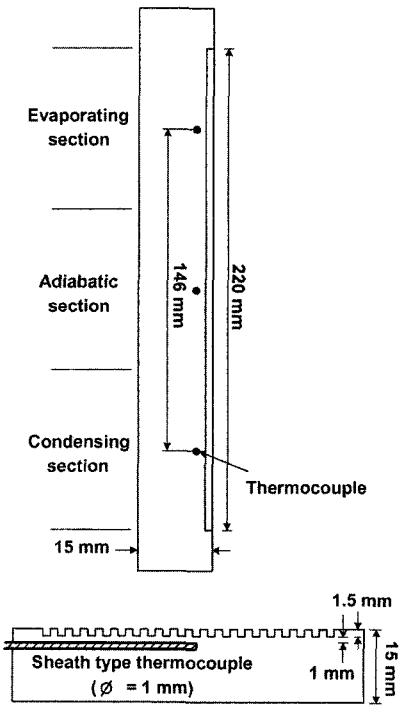

Fig. 3 Locations of thermocouples

the perforated hole and the thermocouple, the silicon compound was injected into the gap of the holes. The distance of temperature sensors that were installed at the evaporating part and condensing part was 146 mm, and the sensor installed at the adiabatic part was in the middle. Also, sheath type thermocouples were installed at the inlet and the outlet of the cooling water system to measure the temperatures of the circulating cooling water. Temperature measurements were conducted using the data logger (DR-230, Yokogawa Co.). All data were processed using the personal computer in real time. The data were measured at a steady state and their average was used for data reduction.

As shown in Fig. 4, to measure the saturation pressure in the test section, two pressure taps of a 1.0 mm diameter were perforated into a flow channel at the evaporating part and condensing part. The pressure sensors (PDCR-961, Druck Co.) were installed. Pressure data were measured using the DAS-1800 (Keithley Co.) at a steady state.

The test section was evacuated to 1×10^{-3} torr by using a high vacuum system, which consists of a rotary and diffusion pump. R-142b was used as the working fluid. The charging cylinder (HPG-10, 96, Taiatsu Co.) of 10 ml was used to charge the working fluid exactly. Also, the charging ratio of the working fluid was changed in turn to 20 vol.%, 40 vol.%, 60 vol.%, and 80 vol.%; the heat flux to the evaporating part was changed in turn to 0.3 W/cm^2, 0.6 W/cm^2, 0.9 W/cm^2, and 1.2 W/cm^2; and the inclination angle to the horizontal orientation was changed in turn to 30°, 60°, and 90°.

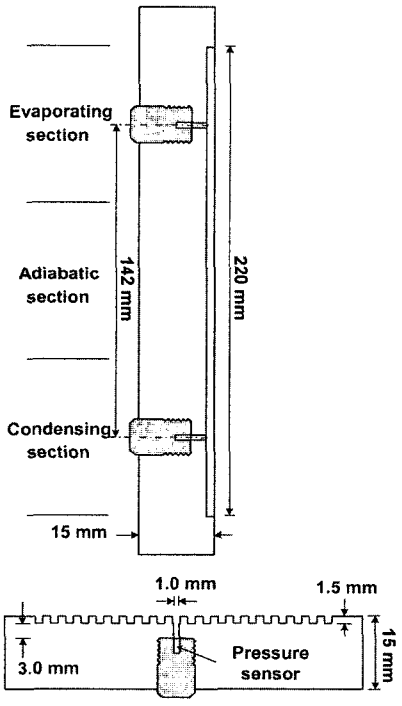

Fig. 4 Locations of pressure sensors

Uncertainty analysis

Temperatures and pressure were monitored in the test loop using the computer and data acquisition system. Each sensor was calibrated to reduce experimental uncertainties before connected to the data logger. The copper-constantan thermocouples with an experimental uncertainty of ±0.2℃ were used for temperature measurements. Pressure transducers were used for measuring the pressure of the working fluid with an estimated accuracy of ±0.2% of the full scale (980 kPa). The pressure read-out uncertainty was 0.3%, and the random uncertainty of pressure measurement was expected to be less than 5%. Hence, the maximum uncertainty for the pressure measurements at the evaporating part and condensing part was 5.5%.

3. Experimental Results and Consideration

3.1 Pressure oscillation characteristics

When the inclination angle to the horizontal orientation (inclination angle, in brief) was 90° and the charging ratio of working fluid (charging ratio, in brief) was changed in turn to 20 vol.%, 40 vol.%, 60 vol.%, and 80 vol.%, the variations of saturation pressure with respect to time at the given heat fluxes and charging ratios were shown in Fig. 5. Generally, as the heat flux to the evaporating part (heat flux, in brief) and the charging ratio was increased, the saturation pressure increased.

At the charging ratio of 20 vol.%, the pressure oscillations (around the average pressure) had complicated forms at the given heat fluxes. There were not abrupt changes in the amplitude of pressure oscillation (oscillation amplitude, in brief) at the heat fluxes of 0.3 W/cm^2 and 0.6 W/cm^2. However, at the heat flux of 0.9 W/cm^2, the oscillation amplitude abruptly changed and the pressure wave became an irregular, non-predictable and unsteady state. This was due to the fact that at the heat flux of 0.3 W/cm^2, the generation and growth of bubbles in the OCHP were anintermittent nucleate boiling process at only some turns among the total flow channels. At the remaining turns of the flow channels, bubbles were almost not generated, and the oscillation phenomenon was not clearly confirmed. As the heat flux was increased to 0.6 W/cm^2, small bubbles generated on the walls (of the channels) in the evaporating part. The bubbles grew and

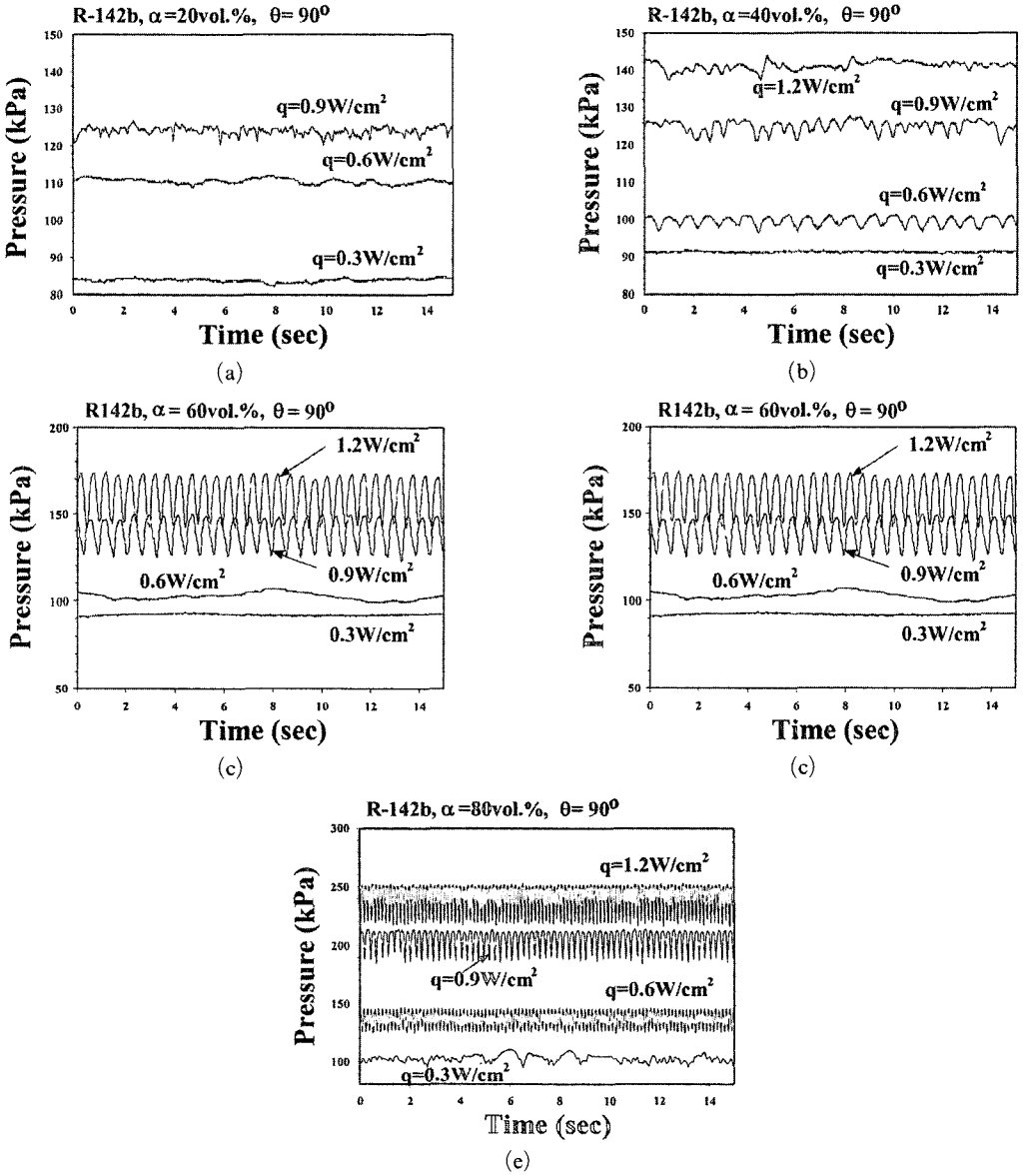

Fig. 5 The variations of saturation pressure in the evaporating part at the given heat fluxes and charging ratios

coalesced to become vapor plugs and the oscillation phenomenon occurred. When the heat flux was increased to 0.9 W/cm^2, the oscillation of vapor plugs and liquid slugs occurred very actively. The movement direction of vapor plugs and liquid slugs changed irregularly in each flow channel. However, as the heat flux was increased, the working fluid supplied to the evaporating part was not sufficient and the dry-out phenomena occurred in some flow channels. Because of the inter-connection of the channels, the working fluid from adjacent flow channels flowed into these channels and the explosion of evaporation occurred on the superheated walls in the evaporating part. Owing to this phenomenon, the saturation pressure abruptly increased and the pressure wave represented an irregular, non-predictable and unsteady state (Kim et al., 1999, 2001 ; Lee et al., 1999a, 1999b).

At the charging ratios of 40 vol.% and 60 vol. %, the pressure oscillation had closed symmetric structures at the given heat fluxes, except the heat flux of 0.3 W/cm^2. The symmetric structure of pressure wave was sinusoidal at the charging ratio of 40 vol.% and the heat flux of 0.6 W/cm^2. When the charging ratio was 60 vol.% and the heat fluxes were 0.6 W/cm^2, 0.9 W/cm^2 and 1.2 W/cm^2, the pressure waves were also sinusoidal. For clarity, an enlarged figure of pressure oscillation at the heat flux of 0.6 W/cm^2 was presented in Fig. 5(d). These states of the OCHP were observed through the flow visualization experiments obtained by Kim et al.(1999), (2001), and Lee et al. (1999a), (1999b). They reported that the steady state operation of the OCHP was observed at the charging ratios of 40 vol.% and 60 vol.%. The active oscillations of working fluid occurred as the symmetric structure of pressure wave was obtained. The oscillation of working fluid was most active when the pressure wave was sinusoidal.

At the charging ratio of 80 vol.%, the pressure waves were also almost symmetric at the given heat fluxes, except the heat flux of 0.3 W/cm^2. Detailed observations showed that the bottom part of the pressure wave has a sharp shape. This was due to the excessive charge of working fluid and the saturation pressure of working fluid increased. It led to an increase in the temperature difference and pressure difference between the evaporating part and condensing part. It was observed that bubbles formed at the evaporating part by nucleate boiling were dissipated in the long liquid slugs shortly before they came to the condensing part. The space vacated by the bubbles was filled by liquid, and the process was repeated. Hence, the bottom part of the pressure waves was sharp and the operating state of the OCHP changed to an unsteady state (Lee et al., 1999b).

In order to analyze the frequency characteristics of pressure oscillation, the signal processing tool using a discrete Fast Fourier Transform (FFT) was applied to obtain the power spectrum of pressure oscillation. The experimentally obtained power spectra of the sinusoidal pressure waveforms at the inclination angle of 90° and the charging ratios of 40 vol.% (heat flux 0.6 W/cm^2 and 0.9 W/cm^2) and 60 vol.% (heat flux 0.9 W/cm^2 and 1.2 W/cm^2) were presented in

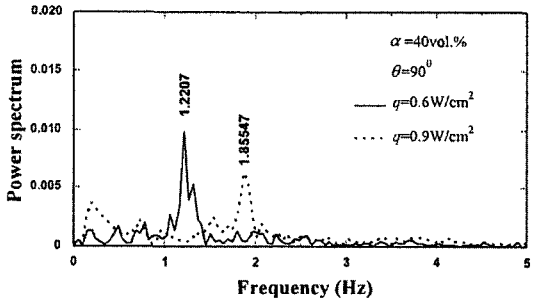

(a) At the charging ratio of 40 vol.%

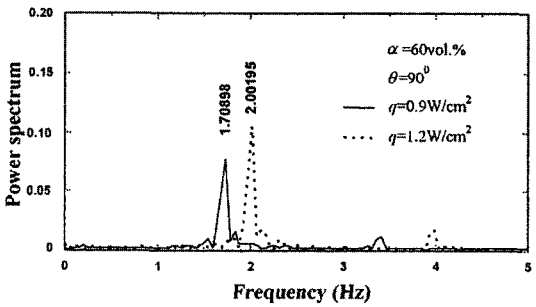

(b) At the charging ratio of 60 vol.%

Fig. 6 The power spectra of the sinusoidal pressure oscillations by the fast Fourier transform

Fig. 6. The dominant frequencies were determined to be 1.2207 Hz and 1.85547 Hz (at the charging ratio of 40 vol.%, Fig. 6(a)) and 1.70898 Hz and 2.00195 Hz (at the charging ratio of 60 vol.%, Fig. 6(b)). As shown in Fig. 6, the value of the dominant frequencies increased with increasing the heat flux and the charging ratio (from 40 vol.% to 60 vol.%).

3.2 Correlation of pressure oscillation and heat transfer characteristics

Figure 7 showed the variation of the effective thermal conductivity with heat flux at the given charging ratios. The effective thermal conductivity was maximal at the charging ratio of 40 vol.%. The experimental results obtained by Kim et al.(1999), (2001), and Lee et al.(1999a), (1999b) also confirmed that the oscillation of working fluid was active at the charging ratio of 40 vol.%. With this charging ratio, the circulation velocity of working fluid was at maximum value, which resulted in the best heat transfer performance.

Figure 8 described the dependence of the effective thermal conductivity, the saturation pressure, the pressure difference, the oscillation amplitude, and the frequency on the given heat fluxes, respectively. Here, the charging ratio was 40 vol.% and the inclination angle was changed in turn to 30°, 60°, and 90°.

As shown in Fig. 8(a), when the inclination

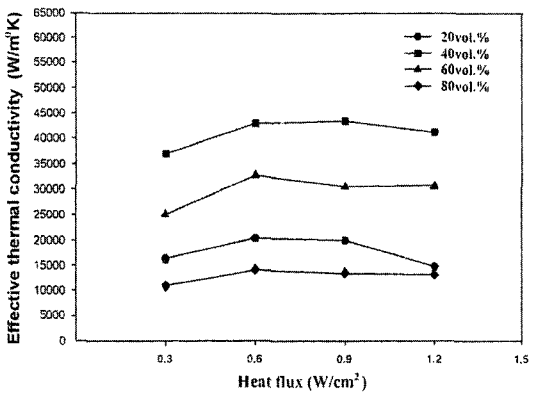

Fig. 7 The variation of the effective thermal conductivity with heat flux at the given charging ratios

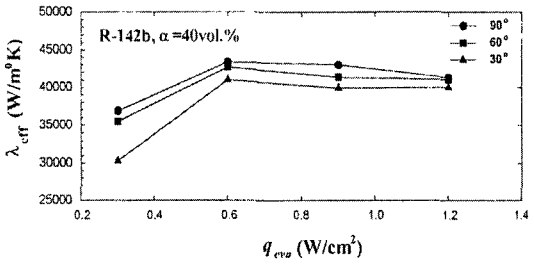

(a) The effective thermal conductivity on heat flux

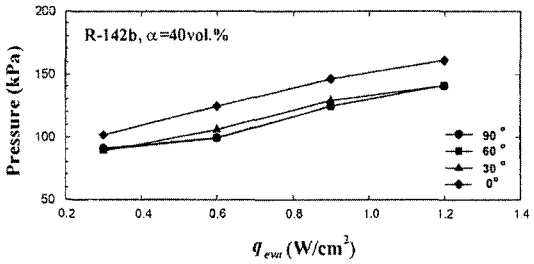

(b) The saturation pressure on heat flux

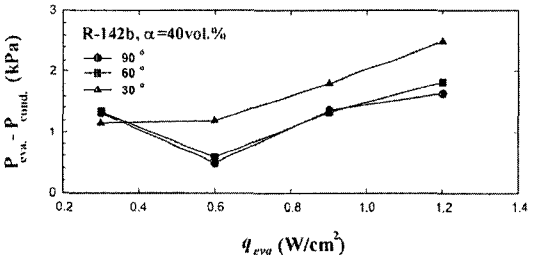

(c) The pressure difference on heat flux

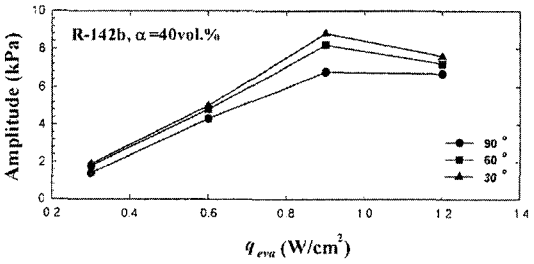

(d) The oscillation amplitude on heat flux

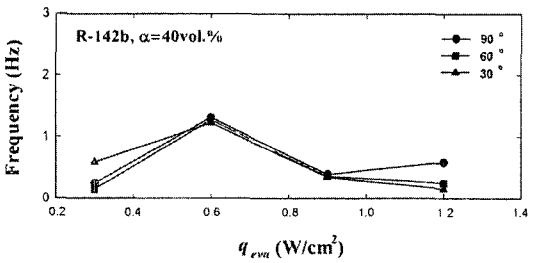

(e) The frequency on heat flux

Fig. 8 The dependence of the various factors on the given heat fluxes [R-142b, α=40 vol.%]

angle was increased, the effective thermal conductivity increased. The effective thermal conductivity was maximal at the inclination angle of 90° and the heat flux of 0.6 W/cm^2. This was due to the fact that when the oscillation of working fluid occurred actively in each flow channel in the OCHP, the pressure oscillation was sinusoidal at the same conditions of the heat flux and charging ratio as mentioned above (see Fig. 5(b)).

The effective thermal conductivity was a representative index to show the performance of the OCHP. The effective thermal conductivity varied according to the working fluid, the charging ratio, the class and shape of the OCHP, the length ratio of the evaporating part and the condensing part, and the inclination angle of the OCHP (Maezawa, 1995).

The effective thermal conductivity λ_{eff} is defined as follows:

$$\lambda_{eff}=\frac{LQ}{A(T_{eva}-T_{cond})} \tag{1}$$

where L is the length from the centre of the evaporating part to that of the condensing part, Q is the heat transfer rate from the evaporating part to the condensing part, A is the total cross sectional area of the channels in the OCHP, and T_{eva} and T_{cond} are the mean surface temperatures of the evaporating part and the condensing part, respectively (Lee et al, 1999b).

Figure 8(b) described the dependence of the saturation pressure on the given heat fluxes. As the heat flux was increased, the saturation pressure linearly increased. At the inclination angle of 0°, because the OCHP almost did not operate at every charging ratio and heat flux condition, when the heat flux was increased, only the saturation pressure ascended. As the inclination angle was increased, the oscillations of working fluid occurred and the saturation pressure decreased. The variation of the saturation pressure was small when the inclination angle was continuously increased. This was due to the influence of surface-tension force which predominated over the gravity force in the flow channels of the OCHP (Lee et al, 1999a).

The dependence of the pressure difference on the given heat fluxes was described in Fig. 8(c). When the inclination angle was decreased, the pressure difference increased. The pressure difference decreased as the heat flux was increased from 0.3 W/cm^2 to 0.6 W/cm^2. However, as the heat flux was increased to more than 0.6 W/cm^2, the pressure difference increased. The pressure difference was at the least when the heat flux was 0.6 W/cm^2 and the inclination angle was 90°. This was due to the symmetric structure of pressure wave which was sinusoidal at the heat flux of 0.6 W/cm^2. When the oscillation of vapor plugs and liquid slugs occurred very actively between the evaporating part and the condensing part, it was observed that a thin liquid film was formed on the walls of the channels. The thin liquid film was generated by the shedding of liquid mass from the tail of liquid slugs during oscillation along the flow channel. By the very rapid oscillation of vapor plugs and liquid slugs along the flow channels, a pseudo slug flow pattern near the annular flow pattern was confirmed shortly after each liquid slug passed. The heat transfer coefficient increased because the thin liquid film decreased the thermal resistance between the surface of the walls and the working fluid. Besides, the bubbles formed within the thin liquid film in the evaporating part separated shortly after they generated from the heated walls. The space vacated by the bubbles was filled by the liquid in the liquid film and the nucleate boiling process continuously occurred. Consequently, the heat transfer coefficient of nucleate boiling and the condensing temperature increased. The condensing pressure increased and the pressure difference was at the least. As the heat flux was continuously increased, the dry-out phenomena occurred and the oscillation of vapor plugs and liquid slugs became slow. Because some of flow channels in the evaporating part started to be filled with vapor, the supply of working fluid to the evaporating part reduced. This led to an increase in the surface temperature of the channels in the evaporating part. The evaporating pressure and the pressure difference increased. Hence, the heat transfer performance decreased. From these results, one can conclude that the pressure difference

is related to the heat transfer performance of the OCHP.

Figure 8(d) showed the dependence of the oscillation amplitude (in the evaporating part) on the given heat fluxes. As the inclination angle was decreased, the oscillation amplitude increased. The oscillation amplitude increased when the heat flux was increased. However, when the heat flux was increased to more than 0.9 W/cm^2, the oscillation amplitude decreased. As mentioned above, the oscillation phenomenon was not clearly confirmed at the heat flux of 0.3 W/cm^2. Therefore, the oscillation amplitude was the least at the heat flux of 0.6 W/cm^2. Also, the pressure oscillation had a sinusoidal waveform at the heat flux of 0.6 W/cm^2 as shown in Fig. 5(b). This implied that the oscillation amplitude was also related to the heat transfer performance of the OCHP.

The influence of the given heat flux and the inclination angles on the frequency of pressure oscillation was shown in Fig. 8(e). When the inclination angle was decreased and the heat flux was increased to more than 0.6 W/cm^2, the frequency decreased. The frequency changed from 0.1 Hz to 1.5 Hz. The frequency was the highest at the heat flux of 0.6 W/cm^2 and the inclination angle of 90°.

The above experimental results showed that the heat transfer performance of the OCHP closely correlated with the characteristics of pressure oscillation occurred in the operating process of the OCHP. At the charging ratio of 40 vol.%, the heat transfer performance was at the best when the inclination angle was 90°, the pressure wave was a sinusoidal waveform, the pressure difference (between the evaporating part and the condensing part) was at the least, the oscillation amplitude was at the least, and the frequency of pressure oscillation was the highest.

4. Conclusions

The following conclusions were obtained through a basic experimental study on the pressure oscillation and heat transfer characteristics of the OCHP.

(1) The frequency of pressure oscillation was between 0.1 Hz and 1.5 Hz at the charging ratio of 40 vol.%.

(2) At the charging ratios of 40 vol.% and 60 vol.%, the dominant frequencies of the sinusoidal pressure oscillations were determined.

(3) The saturation pressure of working fluid in the OCHP increased as the heat flux was increased.

(4) As the charging ratio of working fluid was increased, the amplitude of pressure oscillation increased. When the pressure waves were symmetric sinusoidal waves at the charging ratios of 40 vol.% and 60 vol.%, the heat transfer performance was improved. At the charging ratios of 20 vol.% and 80 vol.%, the waveforms of pressure oscillation were more complicated, and the heat transfer performance reduced.

(5) At the charging ratio of 40 vol.%, the heat transfer performance of the OCHP was at the best when the inclination angle was 90°, the pressure wave was a sinusoidal waveform, the pressure difference was at the least, the oscillation amplitude was at the least, and the frequency of pressure oscillation was the highest.

Acknowledgment

The authors wish to acknowledge the financial support of the Korea Research Foundation made in the program of year of 1998.

References

Akachi, H., 1994, "Looped Capillary Tube Heat Pipe," *Proceedings of 71th General Meeting* conference of JSME, Vol. 3, No. 940~10, pp. 606~611.

Faghri, A., 1995, *Heat Pipe Science And Technology*, Taylor and Francis, Washington, pp. 1~34.

Izumi, T., Gi, K. and Maezawa, S., 1998, "Heat Transfer Characteristics of Double-Ended Closed Oscillating Capillary Tube Heat Pipe," *Journal of JAHP*, Vol. 17, No. 1, pp. 7~11.(in Japanese)

Kim, J. S., Jung, H. S., Kim, J. H. and Kim, J. W., 2001, "Flow Visualization of Oscillation

Characteristics of Liquid and Vapor in Oscillating Capillary Tube Heat Pipe," *The 6th Asian Symposium on Visualization*, Pusan, Korea, pp. 398~401.

Kim, J. S., Lee, W. H., Lee, J. H., Jung, H. S., Kim, J. H. and Jang, J. I., 1999, "Flow Visualization of Oscillating Capillary Tube Heat Pipe," *Proceeding of Thermal Engineering Conference of KSME*, pp. 65~70.(in Korean)

Lee, W. H., Jung, H. S., Kim, J. H. and Kim, J. S., 1999a, "Flow Visualization of Oscillating Capillary Tube Heat Pipe," *11th International Heat Pipe Conference*, Tokyo, Japan, Vol. 2, pp. 131~136.

Lee, W. H., Kim, J. H., Kim, J. S. and Jang, I. S., 1999b, "The Heat Transfer Characteristics of Oscillating Capillary Tube Heat Pipe," *2nd Two-Phase Flow Modelling and Experimentation*, Pisa, Italy, Vol. 3, pp. 1713~1718.

Maezawa, S., 1995, "Working Principle and Thermal Characteristics of Heat Pipe and Thermosyphon," *Journal of JAHP*, Vol. 14, No. 2, pp. 1~11.

Miyazaki, Y. and Akachi, H., 1996, "Heat Transfer Characteristics of Looped Capillary Heat Pipe," *Proceeding of the 5th International Heat Pipe Symposium*, Melbourne, pp. 378~383.

Suzuki, O., 2000-5, "Heat transfer characteristics of a Bubble-Driven Capillary Heat Pipe," *37th National Heat Transfer Symposium of Japan*, pp. 35~36.(in Japanese)